

Chronological changes in soil biogeochemical properties of the glacier foreland of Midtre Lovénbreen, Svalbard, attributed to soil-forming factors

You Jin Kim^a, Dominique Laffly^b, Se-eun Kim^a, Lennart Nilsen^c, Junhwa Chi^a, Sungjin Nam^a, Yong Bok Lee^d, Sujeong Jeong^a, Umakant Mishra^e, Yoo Kyung Lee^a, Ji Young Jung^a

^aKorea Polar Research Institute, 26, Songdomirae-ro, Yeonsu-gu, Incheon 21990, Republic of Korea

^bUniversity of Toulouse 2 Jean Jaurès, Toulouse 31058, France

^cDepartment of Arctic and Marine Biology, University of Tromsø, Framstredet 39, 9019 Tromsø, Norway

^dDivision of Applied Life Science (BK4), Gyeongsang National University, Jinju 52828, Republic of Korea

^eComputational Biology & Biophysics, Sandia National Laboratories, Livermore, CA 94550, United States

Correspondence to: Ji Young Jung

Postal address: 26, Songdomirae-ro, Yeonsu-gu, Incheon 21990, Republic of Korea

Telephone: +82-32-760-5532

Fax: +82-32-760-5509

E-mail: jyjung@kopri.re.kr

Abstract (<300 words)

Glacier forelands provide an excellent opportunity to investigate vegetation succession and soil development along the chronosequence; however, there are few studies on soil biogeochemical changes from environmental factors, aside from time. This study aimed to investigate soil development and biogeochemical changes in the glacier foreland of Midtre Lovénbreen, Svalbard, by considering various factors, including time. Eighteen vegetation and soil variables were measured at 38 different sampling sites of varying soil age, depth, and glacio-fluvial activity. Soil organic matter (SOM) was quantitatively measured, and the compositional changes in SOM were determined following size-density fractionation. In the topsoil, the soil organic carbon (SOC) and total nitrogen (N) content was found to increase along the soil chronosequence and were highly correlated with vegetation-associated variables. These findings suggest that plant-derived material was the main driver of the light fraction of SOM accumulation in the topsoil. The heavy fractions of SOM were composed of microbially transformed organic compounds, eventually contributing to SOM stabilization within short 90-yr deglaciation under harsh climatic conditions. In addition to time, the soil vertical profiles showed that other environmental parameters, also affected the soil biogeochemical properties. The high total phosphorous (P) content and electrical conductivity in the topsoil were attributed to unweathered subglacial materials and a considerable amount of inorganic ions from subglacial meltwater. The high P and magnesium content in the subsoil were attributed to parent materials, while the high sodium and potassium content in the surface soil were a result of sea-salt deposition. Glacio-fluvial runoff hampered ecosystem development by inhibiting vegetation development and SOM accumulation. This study emphasizes the importance of considering various soil-forming factors, including parent/subglacial materials, aeolian deposition, and glacio-fluvial runoff, as well as soil age, to obtain a comprehensive understanding of the ecosystem development in glacier forelands.

Keywords: Glacier foreland; Soil-forming factors; Soil biogeochemical property; Chronosequence; Glacio-fluvial runoff; Svalbard

1. Introduction

Global warming has caused a significant recession of glaciers since the mid-19th century, exposing ice-free land surfaces (Yde et al., 2011). Newly exposed glacier forelands are considered the best place to investigate spatial changes along the chronosequence, as the distance from the glacier edge is a proxy for the age of the land surface (Hågvar, 2012; Schmidt et al., 2008). Thus, the glacier forelands in the Arctic and alpine regions are ideal locations to study the chronological changes in terrestrial ecosystems including vegetation succession, microbial community development, and geochemical weathering (Bekku et al., 2004; Borin et al., 2010; Dong et al., 2016; Hågvar, 2012; Mateos-Rivera et al., 2016; Müller et al., 2012; Nakatsubo et al., 1998; Prach and Rachlewicz, 2012; Uchida et al., 2002; Yde et al., 2011).

Glacier forelands have received considerable attention from soil scientists studying early soil development and soil organic matter (SOM) accumulation, with a focus on chronological changes in soil organic carbon (SOC) and total nitrogen (N) content (Heckmann et al., 2016; Kabala and Zapart, 2012; Nakatsubo et al., 2005; Tanner et al., 2013; Vilmundardóttir et al., 2014a, 2014b). The SOC content has gradually increased within approximately 100-150 years, owing to the increased vegetation cover on the soil surface (Hodkinson et al., 2003; Wietrzyk et al., 2018; Yoshitake et al., 2011). The increase in total N content is largely caused by cyanobacteria during the early stages of soil development and by plant-derived organic debris in the later stages (Mapelli et al., 2011; Pessi et al., 2019; Schmidt et al., 2008). While the quantitative measurement of SOM has been extensively studied, there are a relatively limited number of research on SOM fractionation in deglaciated forelands (Gentsch et al., 2015; Herndon et al., 2017; Khedim et al., 2021; Startsev et al., 2020). For temperate and tropical soils, SOM fractionation based on both size and density is generally used to understand the qualitative properties of SOM, such as mean residence time, microbial accessibility, and carbon sequestration (Lavalée et al., 2020; Six et al., 2002). To date, few studies have investigated the spatial distribution of SOM fractions through size-density fractionation in the glacial forelands (Jílková et al., 2021; Prater et al., 2020); only a handful of these studies have addressed chronological changes in SOM fractions (Schweizer et al., 2018). The variability of each SOM fraction along the chronosequence is required to

provide important information on SOM quality and stability in glacial forelands.

One critical assumption in space-for-time substitution studies is that time is the sole factor influencing soil formation (Dümg et al., 2011; Heckmann et al., 2016; Schmidt et al., 2008). In reality, the biogeochemical properties of glacial foreland soils are not only affected by time but also by parent material, geographic features, and geomorphological disturbances (Anderson, 2007; Bardgett et al., 2005; Szymański et al., 2019; Wojcik et al., 2021; Yde et al., 2011). For example, the total phosphorous (P), calcium (Ca), and magnesium (Mg) in glacier forelands are mainly affected by leaching or weathering of parent bedrock (Andy et al., 2008; D'Amico et al., 2014; Jun et al., 2013). Subglacial materials remaining after deglaciation and aeolian deposits of sea salts have proven to be sources of the various biogeochemical components in foreland soils (ARCUS, 2000; Hallbeck, 2009; Ren et al., 2019; Wojcik et al., 2021; Zeng et al., 2013). Moreover, geomorphological-related processes, particularly glacio-fluvial runoff, may redistribute or remove topsoil materials (Wojcik et al., 2020, 2021). Over time, these various soil-forming factors can create disturbance and heterogeneity in soil profile development in the glacial forelands (Wojcik et al., 2021). Therefore, the knowledge of vertical and horizontal distributions of soil biogeochemical properties is essential to understand the factors influencing soil development.

This study conducted field surveys and laboratory analyses to determine major soil-forming factors and their effects on the soil biogeochemical properties of the Midtre Lovénbreen glacier foreland, in Svalbard. We measured 18 vegetation and soil variables at 38 different sampling sites of varying soil age, depth, and intensity of glacio-fluvial runoff. The objective of this study was to determine chronological changes in the SOC and total N content and their fractions over a ~90 yr deglaciation period. We also determined the horizontal and vertical distributions of soil biogeochemical properties influenced by bedrock, geographic features, and glacio-fluvial runoff. We tested three key hypotheses: 1) SOM accumulation in the topsoil of the glacier foreland is mainly attributed to the plant-derived materials, which may be stabilized through the formation of heavy fractions within a short period, even in harsh climatic conditions; 2) bedrock origin and the surrounding abiotic environment have a great impact on the vertical variability of soil biogeochemical properties; and 3) glacio-fluvial runoff inhibits

soil chronological development.

2. Materials and methods

2.1. Study area

This study was conducted in the Midtre Lovénbreen glacier foreland (78.9 °N, 12.1 °E) on the Brøggerhalvøya Peninsula in northwestern Spitsbergen, Svalbard, Norway (Fig. 1). The bedrock in the Brøggerhalvøya Peninsula is dominated by quartzite, phyllite, red sandstone, and conglomerate, interlayered with marble, limestone, and dolomite (Nilsen et al., 1999; Shi et al., 2018). The rocks consist of quartz, mica, chlorite, feldspar, pyrite, and apatite with additional contributions of carbonate minerals; this has been confirmed through the use of X-ray diffraction (XRD) and Scanning Electron Microscopy-Energy Dispersive Spectroscopy (SEM-EDS) in previous studies (Borin et al., 2010; Koutsopoulou et al., 2010; Mapelli et al., 2011). The average annual temperature and precipitation over the past 30 yr (1981-2020) has been -6 °C and 400-420 mm, respectively (Agnelli et al., 2021; Wietrzyk-Pelka et al., 2021). Following the cessation of the Little Ice Age (1900-1920), the volume of the Midtre Lovénbreen glacier has decreased by approximately 25% (Hansen, 1999; King et al., 2008).

2.2. Sampling strategy and environmental surveys

A total of 35 sampling points were selected from 300 vegetation survey sites studied by Moreau et al. (2005) using a stratified sampling strategy to obtain the most representative samples among previously studied sites. There are five factors considered to select sampling points; the spatial distribution of research points (X-Y coordinates), soil age, glacio-fluvial activity, slope and wind exposure (Moreau et al., 2005). Three additional sites from newly deglaciated areas since the survey by Moreau et al. (2005) were also selected. Soil ages were calculated from high-resolution aerial photographs obtained in 1936, 1966, 1985, 1986, 1999, 2000, and 2013 supplied by the Norwegian Polar Institute. Soil age groups were classified into five intervals: <20, 20-40, 40-60, 60-80, and 80-90 yr (Fig. 1). The information regarding glacio-fluvial characteristics followed the classification by Moreau et al. (2005); active, inactive, and no-runoff areas. The active site experienced high-intensity

and continuous runoff during the melting season in the glacial foreland. The inactive site experienced little glacio-fluvial runoff compared to the active site, although the glacial meltwater continued to form residual flow. The no-runoff site was unaffected by any glacio-fluvial runoff. To determine the effect of glacio-fluvial activities on the glacier foreland, three sites were selected for each active, inactive, and no-runoff site among the 40-60 yr sites (Fig. 1). Over 1,000 ordinary color images (RGB) and near-infrared images were collected from Canon S100 camera to acquire high-resolution topography of the study area and derive vegetation indices such as the normalized difference vegetation index (NDVI) data. In July 2016, the camera was fitted with a near infrared-green-blue (NGB) filter onboard the rotary-wing drone over the study area while flying at a speed of approximately 7 m/s from an altitude of roughly 100 m; along and across track overlaps were set to approximately 70-75%. Pix4D was employed to generate a digital elevation model (DEM) and orthorectified imagery. Corresponding mosaic results were obtained with a ground pixel resolution of approximately 5 cm. Several topographic variables, such as slope and aspect, were extracted from the DEM. The elevation, slope, and aspect did not significantly differ with the soil age and glacio-fluvial activity ($p>0.05$). This indicates that the sampling strategy is able to indicate the changes in vegetation and soil variables by soil age and glacio-fluvial runoff, and exclude the effects from microtopography.

2.3. Vegetation survey

Vegetation observations at each sampling site were conducted in July 2014. Vegetation coverage and frequency of lichen, bryophytes, and vascular plants were measured using a 4 m² quadrat (2 m×2 m) divided into 400 grids (10 cm×10 cm). The coverage was visually estimated by recording the area of ground covered by each plant species within the quadrat. The frequency was determined by calculating the proportion of the grid that plant species were found within the total quadrat. The coverage and frequency of the most dominant vascular plant species (i.e., *Saxifraga oppositifolia* and *Salix polaris*) were measured separately (Moreau et al., 2008). The NDVI was obtained by using the ratio of the difference between reflectance in the near-infrared and red regions of the spectrum and their sum; this index has often been utilized to represent proxy data of the relative greenness of vegetation (Johansen

and Tømmervik, 2014). Although leaves strongly absorb wavelengths of visible light, they strongly reflect wavelengths of near-infrared light. The NDVI was calculated as follows:

$NDVI = \frac{R_{NIR} - R_{red}}{R_{NIR} + R_{red}}$, where R_{NIR} and R_{red} are the reflectance values of the near-infrared and red bands, respectively. The NDVI ranges from -1 to +1, in which dense and vital vegetation approaches +1, while low and scattered vegetation approaches zero (Johansen and Tømmervik, 2014).

2.4. Soil analysis

Soil samples were collected at soil depths of 0-5, 5-10, 10-20, and 20-30 cm over the same period as the vegetation observation. Soil samples were air-dried, passed through a 2 mm sieve, and used for further soil analyses.

The SOC and total N content were determined by a combustion method (950 °C) using an elemental analyzer (EA; FlashEA 1112, Thermo Fisher Scientific, Waltham, MA, USA). Soil samples for SOC analysis were acid washed prior to the EA analysis. The total P, potassium (K), Ca, sodium (Na), and Mg content were determined using an inductively coupled plasma optical mass spectrometer (ICP-OMS; OPTIMA 5300DV, PerkinElmer, Shelton, CT, USA) following digestion with perchloric acid (Kuo, 1996). Soil texture was determined by wet-sieving through a 53 µm sieve after removing SOM with H₂O₂ (34.5%); the silt and clay fractions were quantified using the pipette method. Soil pH and electrical conductivity (EC) were measured using an Orion Star™ A215 (Thermo Fisher Scientific) at soil to deionized water ratios of 1:2 (w/v) and 1:5 (w/v), respectively. To determine SOM quality, the size-density fractionation was carried out using a sodium polytungstate solution (density 1.55 g cm⁻³) and the wet-sieving method (Paré and Bedard-Haughn, 2011; Six et al., 2001; Yoo et al., 2017). A 10 g sample of air-dried soil was mixed with 30 mL of sodium polytungstate solution, and the free-light fraction (FLF) was collected using pre-combusted glass microfiber filters (grade GF/A). The FLF was washed with deionized water several times until the EC had decreased to <5 µS cm⁻¹ (Mueller et al., 2015). The heavy fractions were immersed in water, horizontally shaken for 18 hr, and wet-sieved through a 53 µm sieve. The fraction remaining on the sieve consisted of sand-sized particulate organic matter (SF), while the fraction passing through the sieve were silt/clay-associated SOM (SCF). To

determine the chemical composition of SOM, the SOM fractions (FLF, SF, and SCF) were analyzed at the 3, 8, 36, 57, 70, 77 yr old sites using the double-shot analytical pyrolysis-gas chromatography/mass spectrometry (Py-GC/MS) method (Lee et al., 2020; Mattonai et al., 2020). The SF and SCF were treated with 10% hydrofluoric acid prior to the Py-GC/MS. This analysis was carried out using a furnace-type pyrolyzer (EGA/PY-3030D, Frontier Laboratories Ltd., Koriyama, Japan) connected to a gas chromatograph-mass spectrometer (7890B/5977A, Agilent, Santa Clara, CA, USA); details of the Py-GC/MS operational conditions are listed in Table S1. The pyrolysis products were identified based on the mass spectra of the National Institute of Standard and Technology (NIST) 08 libraries.

2.5. Statistical analysis

Statistical analyses were conducted using the general linear model (GLM), Pearson correlation analysis, and linear regression model with SAS 9.4 (SAS Institute, 2013). We performed an analysis of variance (ANOVA) using the GLM procedure owing to the non-normal distribution of our data; this method can be applied to both balanced and unbalanced data. The fixed variables were soil age, depth, and glacio-fluvial activity. The least-square means were used to test for significant differences in the effects of fixed variables on vegetation and soil data. For the data with significant differences as identified by ANOVA, the Least Significant Difference (LSD) post-hoc test was undertaken to determine differences between specific sites with varying soil age, depth, or glacio-fluvial activity. Pearson's correlation analysis was conducted using SAS 9.4 to determine the relationship between vegetation and soil variables. Linear regression models were created using the regression (REG) procedure to examine the relationship between SOC/total N content and the chemical composition in SOM fractions with soil age. Although generally, a statistical significance level of $p < 0.05$ was applied, statistical tendencies ($p < 0.10$) have also been reported.

3. Results

3.1. Vegetation and soil changes with age

Vegetation and soil biogeochemical properties varied significantly with age (Table 1). Frequency of

S. oppositifolia continued to increase up to 40-60 yr of deglaciation and then decreased thereafter (Fig. 2a). The frequency of *S. polaris* increased significantly and marginally at the 60-80 yr ($p<0.05$) and 80-90 yr sites ($p<0.10$), respectively (Fig. 2b), despite an insignificant increase at the younger sites (<60 yr). As a proxy for total vegetation cover (Johansen and Tømmervik, 2014), the NDVI, increased significantly with soil age (Fig. 2c). Consistently, the SOC and total N content in the upper 5-cm soil showed an increase within the 90-yr deglaciation period (Fig. 2d-e). Soil EC was significantly higher at the youngest (<20 yr) and oldest (80-90 yr) sites compared to the medium-age sites (Fig. 2f). In terms of the correlation between those six variables with significant chronological changes, the SOC and total N content were highly correlated with the frequency of *S. oppositifolia* and *S. polaris* and NDVI (Table 2).

The SOM fractionation showed that the SOC and total N content in the FLF, SCF and SF increased significantly with increasing soil age (Fig. 3a-b). In addition, the Py-GC/MS analysis demonstrated that the relative proportion of lignin-derived aromatic compounds significantly increased in FLF with increasing soil age (Table S2). Moreover, lipid and fatty acid derivatives were more abundant in the SCF and SF over soil age (Table S2).

3.2. Vertical distribution of soil properties

The soil biogeochemical properties of the Midtre Lovénbreen glacier foreland varied vertically (Table 3); the results obtained by the post-hoc test are summarized in Table 4. The SOC and total N content were significantly higher in the topsoil (0-5 cm) than deeper layers (5-30 cm). Higher SOM content at the upper soil depths were significant following 20 yr of glacial retreat, and the total N content increased significantly from the early stage of deglaciation (<20 yr). The total P content at the youngest sites (<20 yr) was significantly higher in the topsoil (0-5 cm) compared to the subsoils (5-30 cm); however, the subsoils of the 40-60 yr sites had a higher P content than the topsoil. Clay content was significantly lower in the surface layer (0-5 cm) relative to deeper layers at the <20 and 20-40 yr sites. Overall, soil pH exceeded 8.0 at the study sites of the glacier foreland, although it was significantly lower in the soil surface (<5 cm) than the deeper layers. The results of elemental analysis showed that the total K and

Na content were higher on the surface than deeper soils; by contrast, the total Mg content tended to increase with soil depth.

3.3. Vegetation and soil changes related to glacio-fluvial runoff

Glacio-fluvial runoff was observed to significantly influence vegetation and soil biogeochemical properties (Table 5). Vegetation frequencies of bryophytes, vascular plants, and *S. oppositifolia* in the active site had significantly decreased by 83-89% compared to those in the no-runoff site; the frequency of lichen also showed a 93% decrease despite there being no significant difference (Fig. 4a). The vegetation frequencies for the inactive site also decreased by 79% compared to the no-runoff site. The SOC and total N content were significantly lower in the active (76%) and inactive (57%) sites, compared to the no-runoff site (Fig. 4b-c). There was a decrease in the SOC and total N content for all SOM fractions in runoff-affected sites. The clay content and soil EC were significantly lower in the active and inactive sites, compared to the no-runoff site (Fig. 4d-e).

4. Discussion

4.1. Vegetation and soil development along the chronosequence

Vegetation succession along the soil chronosequence was observed in the Midtre Lovénbreen glacier foreland, as reported by previous studies (Hodkinson et al., 2003; Moreau et al., 2008; Yoshitake et al., 2011; Müller et al., 2012). As a pioneer species in vegetation succession, *S. oppositifolia* was dominant during the early stage of deglaciation (Moreau et al., 2008; Müller et al., 2012). By contrast, *S. polaris* showed an increase in the frequency at the relatively older sites (>60 yr) of the glacier foreland. This result is consistent with that of Moreau et al. (2008), who found that the frequency of *S. polaris* had remarkably increased after 70 yr of deglaciation. Moreover, the increase in total vegetation cover with increasing soil age, as confirmed by the NDVI, was consistent with previous results for other glacier forelands in Svalbard (Hodkinson et al., 2003; Yoshitake et al., 2011).

The SOC and total N content in the glacier foreland increased with soil age (Fig. 2d-e). The SOC and total N content in the upper 5-cm soil were 1.63 g C kg^{-1} and 0.09 g N kg^{-1} at the youngest site (<20

yr), and 5.15 g C kg⁻¹ and 0.31 g N kg⁻¹ at the oldest site (80-90 yr), respectively. These findings are consistent with a previous study on the Midtre Lovénbreen glacier foreland (Dong et al., 2016), which reported that the SOC and total N content in the upper 10-cm soil increased from 0.3 to 6.9 g C kg⁻¹ and from 0.04 to 0.55 g N kg⁻¹ after 80-yr deglaciation, respectively. By contrast, the SOC and total N content of the Midtre Lovénbreen glacier foreland were significantly lower than other glacier forelands in Svalbard, such as Werenskioldbreen and Irenebreen, where the average SOC and total N content in the upper 5-cm soil were 4.5-22.2 g C kg⁻¹ and 0.2-1.7 g N kg⁻¹, respectively (Kabala and Zapart, 2012; Wietrzyk et al., 2018). Hodkinson et al. (2003) attributed the slow SOM accumulation in the Midtre Lovénbreen glacier foreland to nutrient-poor conditions associated with low temperature and dry conditions. Although climate-derived factors affect the Midtre Lovénbreen and other surrounding glacier forelands (Austre Brøggerbreen, Vestre Lovénbreen and Austre Lovénbreen), the Midtre Lovénbreen foreland experienced the slowest SOM accumulation in particular compared to other glacier forelands (Wietrzyk-Pelka et al., 2020).

Soil EC was higher at the youngest and oldest sites than other-age soils (Fig. 2f). The slightly high EC at the youngest sites (<20 yr) was likely caused by inorganic materials remaining on the soil surface after glacier retreat, such as sulfates, bicarbonates, and dissolved ions in subglacial meltwater (Hallbeck, 2009; Ren et al., 2019). Over time, these inorganic material content might decrease in the soil via erosion, leaching, or plant uptake, leading to lower soil EC (Fig. 2f) (Hallbeck, 2009). However, the EC of the topsoil increased significantly in the oldest sites (80-90 yr), characterized by the highest SOM accumulation (Fig. 2f). This could be attributed to the deposition of sea salts containing soluble/exchangeable ions at the oldest sites that exposed longer and closer to the sea water (Ansari et al., 2013; Zeng et al., 2013). The other possible reason for the higher EC at the 80-90 yr sites than others could be the increasing SOM accumulation with increasing soil age. The SOM with various functional groups can enhance the exchange of ionic substances, eventually increasing soil EC (Adviento-Borbe et al., 2006; Newcomb et al., 2017).

4.2. Compositional changes in soil organic matter

The data presented in Table 2 indicate that surface SOM accumulation along the chronosequence is highly affected by increasing vegetation coverage on the soil surface (Wietrzyk et al., 2018; Yoshitake et al., 2011). This finding is supported by the results of SOM fractionation and Py-GC/MS analysis. The SOC and total N content in the FLF increased significantly with increasing soil age (Fig. 3a-b). The FLF, typically composed of plant leaves and debris, is more susceptible to microbial degradation than SCF and SF fractions, owing to its inherently labile properties or non-protected portions by soil minerals/aggregates (Six et al., 2001; von Lützow et al., 2007; Yang et al., 2012; Zhao et al., 2016). Additionally, the relative proportion of lignin-derived aromatic compounds significantly increased in the FLF with increasing soil age (Table S2). These results confirmed that plant-derived FLF is an essential source of SOM input, causing the accumulation of surface SOC and total N in the deglaciated foreland.

The SOC and total N content in the other SOM fractions (i.e., SCF and SF) had also increased significantly with increasing soil age (Fig. 3a-b). Arctic cryogenic conditions inhibit plant growth and microbial activity (Schulz et al., 2013; Wietrzyk et al., 2018; Yoshitake et al., 2011), restricting SOM accumulation. Nevertheless, the increased SOC and total N content in the SCF and SF reflect the association of microbial metabolites with soil mineral particles along the soil chronosequence (Bernasconi et al., 2011; Dümig et al., 2012; Thomazini et al., 2015). The Py-GC/MS analysis results (Table S2) demonstrated a high abundance of microbially transformed organic compounds, such as lipid and fatty acid derivatives (Yang et al., 2020), in the SCF and SF of the old sites (57, 70 and 77 yr). This indicates that SOM can be stabilized as a mineral-associated form within a short deglaciation period, despite the harsh climatic conditions of the High Arctic (Khedim et al., 2021; Schulz et al., 2013; Thomazini et al., 2015).

4.3. Soil biogeochemical changes by vertical profiles

The SOC and total N content largely derived from vegetation was higher in the topsoil (0-5 cm) than the subsoil (5-30 cm) (Table 4). In the Arctic, most vegetation has a shallow and widespread root system in the topsoil (Wang et al., 2016), leading to the enrichment of SOC and total N content in the soil

surface. As N fixation is an aerobic process, the plant and microbial-available N was particularly higher in the topsoil layer than the deeper layers (Augusto et al., 2017; Tanner et al., 2013). Interestingly, at the young sites (<20 yr), there was no significant difference in SOC content with soil depth, although there was a significant difference in the total N content (Table 4). This is probably because cyanobacteria emerged within 4-5 yr of glacier retreat prior to vegetation establishment, resulting in the earlier development of soil N fixation than SOC accumulation in the topsoil of glacier forelands (Khedim et al., 2021; Mapelli et al., 2011; Pessi et al., 2019; Schmidt et al., 2008; Vries et al., 2021).

The total P content was higher in the soil surface than the deeper layers during the early stage of deglaciation, whereas this vertical gradient gradually reversed following 40 yr of the glacier retreat (Table 4). These results are consistent with the findings for the Hailuogou glacier foreland (Gongga Mountain, Southwest China), where the total P content were higher in the topsoil (0-10 cm) of younger sites (30 yr) and the subsoil (20-50 cm) of older sites (80 and 120 yr), respectively (Jun et al., 2013). At the younger sites, the higher total P content in the topsoil relative to the subsoil was likely a result of the subglacial materials remaining on the soil surface after the glacier retreat (Ren et al., 2019; Wojcik et al., 2020). By contrast, at the older sites (>40 yr), the lower P content in the topsoil than the subsoil was likely to be related to P uptake by plants/microbes for growth or leaching to the subsoil after the glacial retreat (Jun et al., 2013). Additionally, the higher subsoil P content compared to the topsoil with increasing soil age is probably because soil P can be derived from the underlying parent rock materials (Andy et al., 2008; Augusto et al., 2017). Previous studies on the Midtre Lovénbreen glacier foreland reported the existence of apatite that contained elemental P, based on the XRD and SEM-EDS analyses (Borin et al., 2010; Mapelli et al., 2011). Despite no significant chronological effects, the vertical distribution of total P content in the glacier foreland could be explained by subglacial deposits and parent materials.

The clay content tended to decrease in the surface layer (0-5 cm) relative to the deeper layers (Table 4). Water or wind erosion and vertical translocation can remove the fine earth fractions from the surfaces of glacier forelands (Vilmundardóttir et al., 2014b). Kabala and Zapart (2012) reported that snow or glacier melting every spring in the Werenskioldbreen glacier foreland of Svalbard might be the cause

for clay loss in the uppermost soil layer (0-3 cm).

At all sampling sites, soil pH exceeding 8.0 was probably due to marble schist, one of the bedrocks in the Midtre Lovénbreen glacier foreland (Shi et al., 2018; Wietrzyk et al., 2018). However, the lower soil pH in the topsoil compared to the subsoil layers might be attributable to weakly-acidic compounds released from the decomposition of plant-derived FLF (Bernasconi et al., 2011; Vilmundardóttir et al., 2014a; Wietrzyk-Pelka et al., 2020). Meltwater may also cause carbonate leaching every spring, eventually lowering soil pH in the topsoil compared to the subsoil (Kabala and Zapart, 2012).

The higher K and Na content in the topsoil compared to the deeper layers might be explained by the landscape feature of the glacier foreland. The fjord landscape of Svalbard exposes the glacier foreland to oceanic influences, which are then susceptible to wind deposition of the sea salts (ARCUS, 2000; Ansari et al., 2013; Zeng et al., 2013). Conversely, the total Mg content was significantly higher with increasing soil depth (Table 4). Based on mineralogical analysis, parent bedrocks in the Brøggerhalvøya Peninsula primarily contained quartz, mica, chlorite, feldspar, pyrite and apatite (Nilsen et al., 1999; Shi et al., 2018). In particular, SEM-EDX analysis confirmed that Mg was the main element contained in chlorite minerals (Koutsopoulou et al., 2010); this could explain the higher total Mg content in the deeper layers. These results demonstrate that the vertical distribution of soil biogeochemical properties could be influenced not only by vegetation development but also by parent materials and the surrounding abiotic environment.

4.4. Soil biogeochemical changes by glacio-fluvial runoff

Glacio-fluvial runoff considerably increases horizontal heterogeneity of the soils in glacier forelands; however relevant studies are lacking (Wojcik et al., 2021). Previous studies have obtained only limited results, as they have focused only on changes in plant colonization through various glacio-fluvial runoff (Moreau et al., 2008) or have not isolated its effects from topographic factors (Wojcik et al., 2020). Thus, our study is valuable for the acquisition of empirical data on soil biogeochemical changes caused by glacio-fluvial runoff, as it was conducted under controlled soil age and topography.

Vegetation development in the glacier foreland was inhibited by active glacio-fluvial runoff (Fig. 4a),

consistent with the previous study on the Midtre Lovénbreen glacier foreland (Moreau et al., 2008). Meanwhile, the result for inactive site was inconsistent with Moreau et al. (2008), who reported minor impacts from the inactive glacio-fluvial runoff on vegetation frequencies. This might be because we selected the sampling points with no difference in soil age and topographic features among sites of the previous study (Moreau et al., 2008). The glacio-fluvial runoff disturbed the surface SOC and total N accumulation as well as vegetation development (Fig. 4b-c). Among the SOM fractions, a remarkable change in the SOC and total N content was observed for the plant-derived FLF, which was lower in the active (87%) and inactive (78%) sites compared to the no-runoff site. We postulate that runoff can directly restrict soil chronological development by removal of accumulated SOC and total N from the soil surface. In particular, plant-derived FLF is easily removed through glacio-fluvial runoff as a result of its low density (Lavallee et al., 2020; Six et al., 2001). The lack of vegetation development in the active and inactive sites could not protect the soil surface from glacio-fluvial runoff, probably further increasing soil erosion (Church and Ryder, 1972; Gurnell et al., 2000). Moreover, the SOC and total N content of SCF and/or SF were lower in the active and inactive sites, compared to the no-runoff site (Fig. 4b-c), negatively affecting SOM stabilization. This is likely due to the lower clay content in soils affected by glacio-fluvial runoff (Fig. 4d), inhibiting adsorptive interactions between soil particles and SOM (Lavallee et al., 2020; Six et al., 2002). The soil EC, related to the amount of soil inorganic nutrients, was lower in the active and inactive sites compared to the no-runoff site (Fig. 3f). These results contrast with the findings reported by Wojcik et al. (2020), who found that the deposition of SOC and clay particles was enhanced by glacio-fluvial runoff. They explained that, depending on the intensity and frequency, the runoff could erode or deposit soil mineral particles, thereby inhibiting or promoting soil development. Our study was able to empirically confirm that glacio-fluvial runoff retards SOM accumulation and stabilization by removing vegetation cover, clay particles and soil nutrients, eventually inhibiting the ecosystem development in this glacier foreland.

5. Conclusions

This study investigated early soil development in the glacial foreland of Midtre Lovénbreen by

considering various environmental factors as well as time. The results from SOM fractionation and Py-GC/MS analysis revealed that the surface accumulation of FLF along the chronosequence was mainly due to plant-derived material, including lignin-derived aromatic compounds. The increases in the heavy fractions (SCF and SF) and the association of soil mineral particles to organic compounds microbially transformed demonstrated the SOM stabilization within a short period of deglaciation under harsh climatic conditions of the High Arctic. Meanwhile, the vertical soil profile showed that inorganic materials beneath the glacier, parent bedrock, and aeolian deposition important roles as soil-forming factors that determined the soil biogeochemical properties in this region. Lastly, this study was a pioneering attempt to clarify the changes in both vegetation and soil development caused by glacio-fluvial runoff by isolating the effects of time and topography. As a result, the active and inactive sites of glacio-fluvial runoff significantly retarded ecosystem development by inhibiting vegetation establishment and SOM accumulation. Our findings strengthen current interpretations of ecosystem development in glacial forelands by focusing on various soil-forming factors such as soil age and abiotic factors including glacio-fluvial runoff. Finally, we recommend the implementation of additional experiments in various glacial forelands to verify and consolidate the diverse effects of soil-forming factors on vegetation and soil development.

Acknowledgements

This study was supported by Korea Polar Research Institute [KOPRI, PE16030] and by the National Research Foundation of Korea funded by the Korean Government [NRF-2021M1A5A1075508, KOPRI-PN22012]. Contributions of U. Mishra were supported through a U.S. Department of Energy grant to the Sandia National Laboratories, which is a multi-mission laboratory managed and operated by National Technology and Engineering Solutions of Sandia, LLC, a wholly owned subsidiary of Honeywell International, Inc., for the U.S. Department of Energy's National Nuclear Security Administration under contract DE-NA-0003525. Fieldwork was carried out with the approval of the Governor of Svalbard, and the project was registered at the Research in Svalbard Database (RIS-ID: 6752, 10547). We are thankful to the Norwegian Polar Institute for assisting with boat trips in Ny-

Ålesund and to Mr. Peter Park at Angelwing for operating a drone and DEM generation.

References

Adviento-Borbe, M.A.A., Doran, J.W., Drijber, R.A., Dobermann, A., 2006. Soil electrical conductivity and water content affect nitrous oxide and carbon dioxide emissions in intensively managed soils. *J. Environ. Qual.* 35, 1999–2010. <https://doi.org/10.2134/jeq2006.0109>

Agnelli, A., Corti, G., Massaccesi, L., Ventura, S., Acqui, L.P.D., 2021. Impact of biological crusts on soil formation in polar ecosystems. *Geoderma* 401, 115340. <https://doi.org/10.1016/j.geoderma.2021.115340>

Anderson, S.P., 2007. Biogeochemistry of glacial landscape systems. *Annu. Rev. Earth Planet. Sci.* 35, 375–399.

Andy, H., Alexandre M, A., Martyn, T., Andrew, F., Mark, O., John, P., Johanna, L.-P., Brigit, S., 2008. Glacial ecosystems. *Ecol. Monogr.* 78, 41–67.

Ansari, A.H., Hodson, A.J., Heaton, T.H.E., Kaiser, J., Marca-Bell, A., 2013. Stable isotopic evidence for nitrification and denitrification in a High Arctic glacial ecosystem. *Biogeochemistry* 113, 341–357. <https://doi.org/10.1007/s10533-012-9761-9>

ARCUS, 2000. Opportunities for collaboration between the United States and Norway in Arctic research: A workshop report, spring. Fairbanks, Alaska, USA.

Augusto, L., Achat, D.L., Jonard, M., Vidal, D., Ringeval, B., 2017. Soil parent material—A major driver of plant nutrient limitations in terrestrial ecosystems. *Glob. Chang. Biol.* 23, 3808–3824. <https://doi.org/10.1111/gcb.13691>

Bardgett, R.D., Bowman, W.D., Kaufmann, R., Schmidt, S.K., 2005. A temporal approach to linking aboveground and belowground ecology. *Trends Ecol. Evol.* 20, 634–641.

Bekku, Y.S., Nakatubo, T., Kume, A., Koizumi, H., 2004. Soil microbial biomass, respiration rate, and temperature dependence on a successional glacier foreland in Ny-Ålesund, Svalbard. *Arctic, Antarct. Alp. Res.* 36, 395–399.

Bernasconi, S.M., Bauder, A., Bourdon, B., Brunner, I., Bünemann, E., Chris, I., Derungs, N., Edwards, P., Farinotti, D., Frey, B., Frossard, E., Furrer, G., Gierga, M., Göransson, H., Gülland, K., Hagedorn, F., Hajdas, I., Hindshaw, R., Ivy-Ochs, S., Jansa, J., Jonas, T., Kiczka, M., Kretzschmar, R., Lemarchand, E., Luster, J., Magnusson, J., Mitchell, E.A.D., Venterink, H.O., Plötze, M., Reynolds, B., Smittenberg, R.H., Stähli, M., Tamburini, F., Tipper, E.T., Wacker, L., Welc, M., Wiederhold, J.G., Zeyer, J., Zimmermann, S.,

Zumsteg, A., 2011. Chemical and biological gradients along the Damma Glacier soil chronosequence, Switzerland. *Vadose Zo. J.* 10, 867–883. <https://doi.org/10.2136/vzj2010.0129>

Borin, S., Ventura, S., Tambone, F., Mapelli, F., Schubotz, F., Brusetti, L., Scaglia, B., D'Acqui, L.P., Solheim, B., Turicchia, S., Marasco, R., Hinrichs, K.U., Baldi, F., Adani, F., Daffonchio, D., 2010. Rock weathering creates oases of life in a High Arctic desert. *Environ. Microbiol.* 12, 293–303. <https://doi.org/10.1111/j.1462-2920.2009.02059.x>

Church, M., Ryder, J.M., 1972. Paraglacial sedimentation: A consideration of fluvial processes conditioned by glaciation. *Geol. Soc. Ameria Bull.* 83, 3059–3072.

D'Amico, M.E., Freppaz, M., Filippa, G., Zanini, E., 2014. Vegetation influence on soil formation rate in a proglacial chronosequence (Lys Glacier, NW Italian Alps). *Catena* 113, 122–137.

Dong, K., Tripathi, B., Moroenyane, I., Kim, W., Li, N., Chu, H., Adams, J., 2016. Soil fungal community development in a high Arctic glacier foreland follows a directional replacement model, with a mid-successional diversity maximum. *Sci. Rep.* 6, 1–9. <https://doi.org/10.1038/srep26360>

Dümgig, A., Häusler, W., Steffens, M., Kögel-Knabner, I., 2012. Clay fractions from a soil chronosequence after glacier retreat reveal the initial evolution of organo-mineral associations. *Geochim. Cosmochim. Acta* 85, 1–18. <https://doi.org/10.1016/j.gca.2012.01.046>

Dümgig, A., Smittenberg, R., Kögel-Knabner, I., 2011. Concurrent evolution of organic and mineral components during initial soil development after retreat of the Damma glacier, Switzerland. *Geoderma* 163, 83–94. <https://doi.org/10.1016/j.geoderma.2011.04.006>

Gentsch, N., Mikutta, R., Alves, R., Barta, J., Čapek, P., Gittel, A., Hugelius, G., Kuhry, P., Lashchinskiy, N., Palmtag, J., Richter, A., Šantrůčková, H., Schnecker, J., Shibistova, O., Urich, T., Wild, B., Guggenberger, G., 2015. Storage and transformation of organic matter fractions in cryoturbated permafrost soils across the Siberian Arctic 4525–4542. <https://doi.org/10.5194/bg-12-4525-2015>

Gurnell, A.M., Edwards, P.J., Petts, G.E., Ward, J. V., 2000. A conceptual model for alpine proglacial river channel evolution under changing climatic conditions. *Catena* 38, 223–242. [https://doi.org/10.1016/S0341-8162\(99\)00069-7](https://doi.org/10.1016/S0341-8162(99)00069-7)

Hågvar, S., 2012. Primary succession in glacier forelands: How small animals conquer new sand around melting glaciers, in: Young, S. (Ed.), *International Perspectives on Global Environmental Change*. InTech, pp. 151–172. <https://doi.org/10.5772/26536>

Hallbeck, L., 2009. Microbial processes in glaciers and permafrost - A literature study on microbiology affecting

groundwater at ice sheet melting (SKB R-09-37). Swedish Nuclear Fuel and Waste Management Co., Stockholm, Sweden.

Hansen, S. 1999. A photogrammetrical, climate-statistical and geomorphological approach to the post Little Ice age changes of the Midtre Lovénbreen glacier, Svalbard. Master thesis, Univ. Copenhagen-The University Courses on Svalbard (UNIS)-University of Tromsø, Norway.

Heckmann, T., Mccoll, S., Morche, D., 2016. Retreating ice: Research in pro-glacial areas matters. *Earth Surf. Process. Landforms* 41, 271–276. <https://doi.org/10.1002/esp.3858>

Herndon, E., Albashaireh, A., Singer, D., Roy, T., Gu, B., Graham, D., 2017. Influence of iron redox cycling on organo-mineral associations in Arctic tundra soil. *Geochim. Cosmochim. Acta* 207, 210–231. <https://doi.org/10.1016/j.gca.2017.02.034>

Hodkinson, I.D., Coulson, S.J., Webb, N.R., 2003. Community assembly along proglacial chronosequences in the high Arctic: Vegetation and soil development in north-west Svalbard. *J. Ecol.* 91, 651–663. <https://doi.org/10.1046/j.1365-2745.2003.00786.x>

Jílková, V., Devetter, M., Bryndová, M., Hájek, T., 2021. Carbon sequestration related to soil physical and chemical properties in the high Arctic global biogeochemical cycles. *Global Biogeochem. Cycles* 35, 1–15. <https://doi.org/10.1029/2020GB006877>

Johansen, B., Tømmervik, H., 2014. The relationship between phytomass, NDVI and vegetation communities on Svalbard. *Int. J. Appl. Earth Obs. Geoinf.* 27, 20–30. <https://doi.org/10.1016/j.jag.2013.07.001>

Jun, Z., Yanhong, W., Jörg, P., Haijian, B., Dong, Y., Shouqin, S., LuoJi, Hongyang, S., 2013. Changes of soil phosphorus speciation along a 120-year soil chronosequence in the Hailuogou Glacier retreat area (Gongga Mountain, SW China). *Geoderma* 195–196, 251–259. <https://doi.org/10.1016/j.geoderma.2012.12.010>

Kabala, C., Zapart, J., 2012. Initial soil development and carbon accumulation on moraines of the rapidly retreating Werenskiold Glacier, SW Spitsbergen, Svalbard archipelago. *Geoderma* 175–176, 9–20. <https://doi.org/10.1016/j.geoderma.2012.01.025>

Khedim, N., Cécillon, L., Poulenard, J., Barré, P., Baudin, F., Marta, S., Rabaté, A., Dentant, C., Cauvy-Fraunié, S., Anthelme, F., Gielly, L., Ambrosini, R., Franzetti, A., Azzoni, R.S., Caccianiga, M.S., Compostella, C., Clague, J., Tielidze, L., Messager, E., Choler, P., Ficetola, G.F., 2021. Topsoil organic matter build-up in glacier forelands around the world. *Glob. Chang. Biol.* 27, 1662–1677. <https://doi.org/10.1111/gcb.15496>

King, E.C., Smith, A.M., Murray, T., Stuart, G.W., 2008. Glacier-bed characteristics of Midtre Lovénbreen,

Svalbard, from high-resolution seismic and radar surveying. *J. Glaciol.* 54, 145–156.
<https://doi.org/10.3189/002214308784409099>

Koutsopoulou, E., Papoulis, D., Tsolis-Katagas, P., Kornaros, M., 2010. Clay minerals used in sanitary landfills for the retention of organic and inorganic pollutants. *Appl. Clay Sci.* 49, 372–382.
<https://doi.org/10.1016/j.clay.2010.05.004>

Kuo, S., 1996. Phosphorus, in: Sparks, D.L. (Ed.), *Methods of soil analysis Part 3: Chemical methods*. American Society of Agronomy and Soil Science Society of America, Madison, USA, pp. 569–919.

Lavallee, J.M., Soong, J.L., Cotrufo, M.F., 2020. Conceptualizing soil organic matter into particulate and mineral-associated forms to address global change in the 21st century. *Glob. Chang. Biol.* 26, 261–273.
<https://doi.org/10.1111/gcb.14859>

Lee, H., Jae, J., Lee, H.W., Park, S., Jeong, J., Lam, S.S., Park, Y.K., 2020. Production of bio-oil with reduced polycyclic aromatic hydrocarbons via continuous pyrolysis of biobutanol process derived waste lignin. *J. Hazard. Mater.* 384, 121231. <https://doi.org/10.1016/j.jhazmat.2019.121231>

Mapelli, F., Marasco, R., Rizzi, A., Baldi, F., Ventura, S., Daffonchio, D., Borin, S., 2011. Bacterial communities involved in soil formation and plant establishment triggered by pyrite bioweathering on Arctic moraines. *Microb. Ecol.* 61, 438–447. <https://doi.org/10.1007/s00248-010-9758-7>

Mateos-Rivera, A., Yde, J.C., Wilson, B., Finster, K.W., Reigstad, L.J., Øvreås, L., 2016. The effect of temperature change on the microbial diversity and community structure along the chronosequence of the sub-arctic glacier forefield of Styggedalsbreen (Norway). *FEMS Microbiol. Ecol.* 92, 1–13.
<https://doi.org/10.1093/femsec/fiw038>

Mattonai, M., Watanabe, A., Ribechini, E., 2020. Characterization of volatile and non-volatile fractions of spices using evolved gas analysis and multi-shot analytical pyrolysis. *Microchem. J.* 159, 105321.
<https://doi.org/10.1016/j.microc.2020.105321>

Moreau, M., Laffly, D., Joly, D., Brossard, T., 2005. Analysis of plant colonization on an arctic moraine since the end of the Little Ice Age using remotely sensed data and a Bayesian approach. *Remote Sens. Environ.* 99, 244–253.

Moreau, M., Mercier, D., Laffly, D., Roussel, E., 2008. Impacts of recent paraglacial dynamics on plant colonization: A case study on Midtre Lovénbreen foreland, Spitsbergen (79°N). *Geomorphology* 95, 48–60.
<https://doi.org/10.1016/j.geomorph.2006.07.031>

Mueller, C.W., Rethemeyer, J., Kao-Kniffin, J., Löppmann, S., Hinkel, K.M., Bockheim, J.G., 2015. Large amounts of labile organic carbon in permafrost soils of northern Alaska. *Glob. Chang. Biol.* 21, 2804–2817. <https://doi.org/10.1111/gcb.12876>

Müller, E., Eidesen, P.B., Ehrlich, D., Alsos, I.G., 2012. Frequency of local, regional, and long-distance dispersal of diploid and tetraploid *Saxifraga oppositifolia* (*Saxifragaceae*) to Arctic glacier forelands. *Am. J. Bot.* 99, 459–471. <https://doi.org/10.3732/ajb.1100363>

Nakatsubo, T., Bekku, Y., Kume, A., Koizumi, H., 1998. Respiration of the belowground parts of vascular plants: Its contribution to total soil respiration on a successional glacier foreland in Ny-Ålesund, Svalbard. *Polar Res.* 17, 53–60. <https://doi.org/10.1111/j.1751-8369.1998.tb00258.x>

Nakatsubo, T., Bekku, Y.S., Uchida, M., Muraoka, H., Kume, A., Ohtsuka, T., Masuzawa, T., Kanda, H., Koizumi, H., 2005. Ecosystem development and carbon cycle on a glacier foreland in the high Arctic, Ny-Ålesund, Svalbard. *J. Plant Res.* 118, 173–179. <https://doi.org/10.1007/s10265-005-0211-9>

Newcomb, C.J., Qafoku, N.P., Grate, J.W., Bailey, V.L., De Yoreo, J.J., 2017. Developing a molecular picture of soil organic matter-mineral interactions by quantifying organo-mineral binding. *Nat. Commun.* 8. <https://doi.org/10.1038/s41467-017-00407-9>

Nilsen, L., Brossard, T., Joly, D., 1999. Mapping plant communities in a local Arctic landscape applying a scanned infrared aerial photograph in a geographical information system. *Int. J. Remote Sens.* 20, 463–480. <https://doi.org/10.1080/014311699213541>

Paré, M.C., Bedard-Haughn, A., 2011. Optimum liquid density in separation of the physically uncomplexed organic matter in Arctic soils. *Can. J. Soil Sci.* 91, 65–68. <https://doi.org/10.4141/CJSS10051>

Pessi, I.S., Pushkareva, E., Lara, Y., Borderie, F., Wilmotte, A., Elster, J., 2019. Marked succession of cyanobacterial communities following glacier retreat in the high Arctic. *Microb. Ecol.* 77, 136–147. <https://doi.org/10.1007/s00248-018-1203-3>

Prach, K., Rachlewicz, G., 2012. Succession of vascular plants in front of retreating glaciers in central Spitsbergen. *Polish Polar Res.* 33, 319–328. <https://doi.org/10.2478/v10183-012-0022-3>

Prater, I., Zubrzycki, S., Buegger, F., Zoor-Füllgraff, L.C., Angst, G., 2020. From fibrous plant residues to mineral-associated organic carbon – the fate of organic matter in Arctic permafrost soils. *Biogeosciences* 17, 3367–3383. <https://doi.org/10.5194/bg-17-3367-2020>

Ren, Z., Martyniuk, N., Oleksy, I.A., Swain, A., Hotaling, S., 2019. Ecological stoichiometry of the mountain cryosphere. *Front. Ecol. Evol.* 7, 360.

Schmidt, S.K., Reed, S.C., Nemergut, D.R., Grandy, A.S., Cleveland, C.C., Weintraub, M.N., Hill, A.W., Costello, E.K., Meyer, A.F., Neff, J.C., Martin, A.M., 2008. The earliest stages of ecosystem succession in high-elevation (5000 metres above sea level), recently deglaciated soils. *Proc. R. Soc. B Biol. Sci.* 275, 2793–2802. <https://doi.org/10.1098/rspb.2008.0808>

Schulz, S., Brankatschk, R., Dümig, A., Kögel-Knabner, I., Schloter, M., Zeyer, J., 2013. The role of microorganisms at different stages of ecosystem development for soil formation. *Biogeosciences* 10, 3983–3996. <https://doi.org/10.5194/bg-10-3983-2013>

Schweizer, S.A., Hoeschen, C., Schlüter, S., Kögel-Knabner, I., Mueller, C.W., 2018. Rapid soil formation after glacial retreat shaped by spatial patterns of organic matter accrual in microaggregates. *Glob. Chang. Biol.* 24, 1637–1650. <https://doi.org/10.1111/gcb.14014>

Shi, F., Shi, X., Su, X., Fang, X., Wu, Y., Cheng, Z., Yao, Z., 2018. Clay minerals in Arctic Kongsfjorden surface sediments and their implications on provenance and paleoenvironmental change. *Acta Oceanol. Sin.* 37, 29–38. <https://doi.org/10.1007/s13131-018-1220-6>

Six, J., Conant, R.T., Paul, E.A., Paustian, K., 2002. Stabilization mechanisms of SOM implications for C saturation of soils. *Plant Soil* 241, 155–176.

Six, J., Guggenberger, G., Paustian, K., Haumaier, L., Elliott, E.T., Zech, W., 2001. Sources and composition of soil organic matter fractions between and within soil aggregates. *Eur. J. Soil Sci.* 52, 607–618. <https://doi.org/10.1046/j.1365-2389.2001.00406.x>

Startsev, V. V., Khaydapova, D.D., Degteva, S. V., Dymov, A.A., 2020. Soils on the southern border of the cryolithozone of European part of Russia (the Subpolar Urals) and their soil organic matter fractions and rheological behavior. *Geoderma* 361, 114006. <https://doi.org/10.1016/j.geoderma.2019.114006>

Szymański, W., Maciejowski, W., Ostafin, K., Ziaja, W., Sobucki, M., 2019. Impact of parent material, vegetation cover, and site wetness on variability of soil properties in proglacial areas of small glaciers along the northeastern coast of Sørkappland (SE Spitsbergen). *Catena* 183, 104209. <https://doi.org/10.1016/j.catena.2019.104209>

Tanner, L.H., Walker, A.E., Nivison, M., Smith, D.L., 2013. Changes in soil composition and floral coverage on a glacial foreland chronosequence in southern Iceland. *Open J. Soil Sci.* 3, 191–198. <https://doi.org/10.4236/ojss.2013.34022>

Thomazini, A., Mendonça, E.S., Teixeira, D.B., Almeida, I.C.C., La Scala, N., Canellas, L.P., Spokas, K.A., Milori, D.M.B.P., Turbay, C.V.G., Fernandes, R.B.A., Schaefer, C.E.G.R., 2015. CO₂ and N₂O emissions in

a soil chronosequence at a glacier retreat zone in Maritime Antarctica. *Sci. Total Environ.* 521–522, 336–345. <https://doi.org/10.1016/j.scitotenv.2015.03.110>

Uchida, M., Muraoka, H., Nakatsubo, T., Bekku, Y., Ueno, T., Kanda, H., Koizumi, H., 2002. Net photosynthesis, respiration, and production of the moss *Sanionia uncinata* on a glacier foreland in the High Arctic, Ny-Ålesund, Svalbard. *Arctic, Antarct. Alp. Res.* 34, 287–292.
<https://doi.org/10.1080/15230430.2002.12003496>

Vilmundardóttir, O.K., Gísladóttir, G., Lal, R., 2014a. Early stage development of selected soil properties along the proglacial moraines of Skaftafellsjökull glacier, SE-Iceland. *Catena* 121, 142–150.
<https://doi.org/10.1016/j.catena.2014.04.020>

Vilmundardóttir, O.K., Gísladóttir, G., Lal, R., 2014b. Soil carbon accretion along an age chronosequence formed by the retreat of the Skaftafellsjökull glacier, SE-Iceland. *Geomorphology* 228, 124–133.
<https://doi.org/10.1016/j.geomorph.2014.08.030>

von Lützow, M., Kögel-Knabner, I., Ekschmitt, K., Flessa, H., Guggenberger, G., Matzner, E., Marschner, B., 2007. SOM fractionation methods: Relevance to functional pools and to stabilization mechanisms. *Soil Biol. Biochem.* 39, 2183–2207. <https://doi.org/10.1016/j.soilbio.2007.03.007>

Vries, F.T. De, Thion, C., Bahn, M., Pinto, B.B., Cécillon, S., Frey, B., Grant, H., Nicol, G.W., Wanek, W., Prosser, J.I., Bardgett, R.D., 2021. Glacier forelands reveal fundamental plant and microbial controls on short-term ecosystem nitrogen retention. *J. Ecol.* 00, 1–14. <https://doi.org/10.1111/1365-2745.13748>

Wang, P., Mommer, L., van Ruijven, J., Berendse, F., Maximov, T.C., Heijmans, M.M.P.D., 2016. Seasonal changes and vertical distribution of root standing biomass of graminoids and shrubs at a Siberian tundra site. *Plant Soil* 407, 55–65. <https://doi.org/10.1007/s11104-016-2858-5>

Wietrzyk-Pełka, P., Rola, K., Patchett, A., Szymański, W., Węgrzyn, M.H., Björk, R.G., 2021. Patterns and drivers of cryptogam and vascular plant diversity in glacier forelands. *Sci. Total Environ.* 770, 144793.
<https://doi.org/10.1016/j.scitotenv.2020.144793>

Wietrzyk-Pełka, P., Rola, K., Szymański, W., Węgrzyn, M.H., 2020. Organic carbon accumulation in the glacier forelands with regard to variability of environmental conditions in different ecogenesis stages of High Arctic ecosystems. *Sci. Total Environ.* 717, 1–12. <https://doi.org/10.1016/j.scitotenv.2019.135151>

Wietrzyk, P., Rola, K., Osyczka, P., Nicia, P., Szymański, W., Węgrzyn, M., 2018. The relationships between soil chemical properties and vegetation succession in the aspect of changes of distance from the glacier forehead and time elapsed after glacier retreat in the Irenebreen foreland (NW Svalbard). *Plant Soil* 428,

195–211. <https://doi.org/10.1007/s11104-018-3660-3>

Wojcik, R., Donhauser, J., Frey, B., Benning, L.G., 2020. Time since deglaciation and geomorphological disturbances determine the patterns of geochemical, mineralogical and microbial successions in an Icelandic foreland. *Geoderma* 379, 114578. <https://doi.org/10.1016/j.geoderma.2020.114578>

Wojcik, R., Eichel, J., Bradley, J.A., Benning, L.G., 2021. How allogenic factors affect succession in glacier forefields. *Earth-Science Rev.* 218, 103642. <https://doi.org/10.1016/j.earscirev.2021.103642>

Yang, J., Li, A., Yang, Y., Li, G., Zhang, F., 2020. Soil organic carbon stability under natural and anthropogenic-induced perturbations. *Earth-Science Rev.* 205, 103199. <https://doi.org/10.1016/j.earscirev.2020.103199>

Yang, X., Ren, W., Sun, B., Zhang, S., 2012. Effects of contrasting soil management regimes on total and labile soil organic carbon fractions in a loess soil in China. *Geoderma* 177–178, 49–56. <https://doi.org/10.1016/j.geoderma.2012.01.033>

Yde, J.C., Bárcena, T.G., Finster, K.W., 2011. Subglacial and Proglacial Ecosystem Responses to Climate Change, in: Blanco, J. (Ed.), *Climate Change - Geophysical Foundations and Ecological Effects*. InTech, pp. 459–478. <https://doi.org/10.5772/24236>

Yoo, G., Kim, H., Choi, J.Y., 2017. Soil aggregate dynamics influenced by biochar addition using the ¹³C natural abundance method. *Soil Sci. Soc. Am. J.* 81, 612–621. <https://doi.org/10.2136/sssaj2016.09.0313>

Yoshitake, S., Uchida, M., Ohtsuka, T., Kanda, H., Koizumi, H., Nakatubo, T., 2011. Vegetation development and carbon storage on a glacier foreland in the High Arctic, Ny-Ålesund, Svalbard. *Polar Sci.* 5, 391–397. <https://doi.org/10.1016/j.polar.2011.03.002>

Zeng, Y.X., Yan, M., Yu, Y., Li, H.R., He, J.F., Sun, K., Zhang, F., 2013. Diversity of bacteria in surface ice of Austre Lovénbreen glacier, Svalbard. *Arch. Microbiol.* 195, 313–322. <https://doi.org/10.1007/s00203-013-0880-z>

Zhao, S., Li, K., Zhou, W., Qiu, S., Huang, S., He, P., 2016. Changes in soil microbial community, enzyme activities and organic matter fractions under long-term straw return in north-central China. *Agric. Ecosyst. Environ.* 216, 82–88. <https://doi.org/10.1016/j.agee.2015.09.028>

Table 1. Analysis of variance (ANOVA) examining the effect of soil age on vegetation and soil biogeochemical properties (soil depth = 0-5 cm)

Vegetation frequency						
	Lichens	Bryophytes	Vascular plant	<i>Saxifraga oppositifolia</i>	<i>Salix polaris</i>	NDVI
Soil age	0.496	0.290	0.100	<0.001**	0.010**	0.008**
	SOC	Total N	Total P	Sand	Silt	Clay
	0.074*	0.036*	0.586	0.423	0.274	0.797
	pH	EC	K	Ca	Na	Mg
	0.189	0.095*	0.620	0.737	0.354	0.136

Bold numbers with ** and * denote significance at p<0.05 and p<0.10, respectively.

Table 2. Correlation coefficient (r) of vegetation and soil variables with soil age (soil depth = 0-5 cm).

	<i>Salix polaris</i>	NDVI	SOC	Total N	EC
<i>Saxifraga oppositifolia</i>	0.097	0.338*	0.350**	0.308*	-0.268
<i>Salix polaris</i>	1	0.251	0.463**	0.464**	-0.038
NDVI		1	0.557**	0.567**	0.095
SOC			1	0.873**	0.087
Total N				1	0.076
EC					1

** and * denote significance at $p<0.05$ and $p<0.10$, respectively.

Bold numbers denote moderate or strong correlation ($r>0.4$).

Table 3. Analysis of variance (ANOVA) examining the effect of soil depth on soil biogeochemical properties.

	Age	SOC	Total N	Total P	Sand	Silt	Clay	pH	EC	K	Ca	Na	Mg
Soil depth	<20 yr	0.146	0.048**	0.059*	0.169	0.258	0.073*	0.094*	0.489	<0.001**	0.597	<0.001**	0.898
	20-40 yr	0.028**	0.073*	0.994	0.366	0.843	0.041**	0.038**	0.146	<0.001**	0.239	0.469	0.082*
	40-60 yr	<0.001**	<0.001**	0.582	0.463	0.643	0.233	<0.001**	0.282	<0.001**	0.718	0.161	<0.001**
	60-80 yr	<0.001**	<0.001**	0.088*	0.971	0.955	0.986	0.002**	0.504	<0.001**	0.319	<0.001**	<0.001**
	80-90 yr	<0.001**	0.001**	0.950	0.829	0.866	0.829	0.001**	0.988	<0.001**	0.842	0.149	0.040**

Bold numbers with ** and * denote significance at p<0.05 and p<0.10, respectively.

Table 4. Vertical distribution of soil biogeochemical properties.

Age	Soil depth	SOC	Total N	Total P	Clay	pH	K	Na	Mg
		----- g kg ⁻¹ soil -----	----- % -----	----- g kg ⁻¹ soil -----	-----	-----	-----	-----	-----
<20 yr	0-5 cm	1.63 (0.41)	0.09^b (0.02)	0.33^b (0.03)	8.6 ^a (3.0)	8.5 ^a (0.1)	12.39^b (1.15)	0.55^b (0.05)	6.25 (1.14)
	5-10 cm	0.96 (0.05)	0.04^a (<0.01)	0.25^a (0.01)	13.9 ^b (0.5)	8.7 ^b (<0.1)	3.66^a (0.02)	0.17^a (0.01)	6.71 (0.46)
	10-20 cm	0.93 (0.12)	0.04^a (<0.01)	0.29^{ab} (0.01)	15.1 ^b (0.4)	8.7 ^b (<0.1)	4.17^a (0.20)	0.19^a (0.01)	6.83 (0.20)
	20-30 cm	0.98 (0.10)	0.06^{ab} (<0.01)	0.27^a (<0.01)	13.7 ^b (0.2)	8.7 ^{ab} (<0.1)	3.86^a (0.07)	0.15^a (0.01)	6.38 (0.16)
20-40 yr	0-5 cm	2.66^b (0.54)	0.18^b (0.05)	0.31 (0.06)	5.3 ^a (1.2)	8.1 ^a (0.1)	10.64^b (1.70)	0.22 (0.08)	4.56^a (0.91)
	5-10 cm	1.49^a (0.13)	0.11^{ab} (0.03)	0.32 (0.02)	9.3 ^{ab} (1.7)	8.5^b (0.1)	3.98^a (0.58)	0.14 (0.01)	7.96^b (1.22)
	10-20 cm	1.34^a (0.13)	0.08^a (0.01)	0.30 (0.01)	11.6^b (1.4)	8.5^b (0.1)	4.15^a (0.38)	0.14 (0.01)	7.52^b (0.89)
	20-30 cm	1.55^a (0.23)	0.09^a (0.02)	0.31 (0.01)	11.2^b (1.8)	8.7^b (0.1)	3.94^a (0.30)	0.14 (0.01)	7.31^b (0.67)
40-60 yr	0-5 cm	4.47^b (0.76)	0.25^b (0.04)	0.30 (0.04)	6.7 (1.2)	8.3^a (0.1)	9.51^b (0.69)	0.35 (0.09)	3.57^a (0.49)
	5-10 cm	1.82^a (0.19)	0.11^a (0.02)	0.32 (0.02)	9.1 (1.3)	8.6^b (<0.1)	3.53^a (0.22)	0.23 (0.10)	6.90^b (0.28)
	10-20 cm	1.66^a (0.16)	0.10^a (0.02)	0.33 (0.03)	9.5 (1.2)	8.7^b (<0.1)	3.79^a (0.17)	0.16 (0.02)	7.11^b (0.29)
	20-30 cm	1.59^a (0.19)	0.09^a (0.02)	0.38 (0.07)	10.1 (1.2)	8.7^b (<0.1)	4.03^a (0.20)	0.15 (0.01)	6.99^b (0.28)
60-80 yr	0-5 cm	5.17^b (0.73)	0.36^b (0.05)	0.24^a (0.03)	7.0 (1.8)	8.2^a (0.1)	10.91^b (1.24)	0.55^b (0.12)	3.49^a (0.46)
	5-10 cm	2.18^a (0.48)	0.10^a (0.02)	0.30^{ab} (0.02)	7.5 (1.8)	8.5^b (0.1)	4.29^a (0.39)	0.20^a (0.02)	6.99^b (0.31)
	10-20 cm	1.78^a (0.40)	0.08^a (0.01)	0.28^{ab} (0.02)	7.9 (1.8)	8.6^b (0.1)	3.82^a (0.21)	0.19^a (0.02)	6.82^b (0.20)
	20-30 cm	1.67^a (0.25)	0.07^a (0.01)	0.34^b (0.04)	7.7 (1.4)	8.6^b (0.1)	4.62^a (0.41)	0.20^a (0.04)	7.52^b (0.33)
80-90 yr	0-5 cm	5.15^b (1.12)	0.31^b (0.07)	0.35 (0.06)	5.6 (1.6)	8.1^a (0.1)	10.96^b (1.13)	0.53 (0.21)	4.41^a (0.74)
	5-10 cm	1.62^a (0.09)	0.09^a (0.01)	0.37 (0.07)	6.8 (2.3)	8.4^b (0.1)	4.22^a (0.45)	0.23 (0.04)	7.92^b (1.08)
	10-20 cm	1.47^a (0.13)	0.08^a (0.01)	0.32 (0.03)	8.0 (2.1)	8.5^b (0.1)	4.04^a (0.37)	0.21 (0.04)	7.80^b (1.07)
	20-30 cm	1.40^a (0.13)	0.07^a (0.01)	0.36 (0.06)	7.7 (2.0)	8.5^b (0.1)	4.10^a (0.46)	0.23 (0.04)	7.24^b (0.62)

Bold numbers with different letters in shaded cells denote significant difference at p<0.05 using the post-hoc test.

Table 5. Analysis of variance (ANOVA) examining the effect of glacial-fluvial runoff on vegetation and soil biogeochemical properties (soil depth = 0-5 cm).

Glacial- fluvial runoff	Vegetation frequency					NDVI
	Lichens	Bryophytes	Vascular plant	<i>Saxifraga oppositifolia</i>	<i>Salix polaris</i>	
	0.372	0.061*	0.044**	0.002**	0.606	0.494
SOC	Total N	Total P	Sand	Silt	Clay	
0.034**	0.019**	0.600	0.209	0.325	0.014**	
pH	EC	K	Ca	Na	Mg	
0.182	0.036**	0.866	0.219	0.338	0.230	

Bold numbers with ** and * denote significance at p<0.05 and p<0.10, respectively.

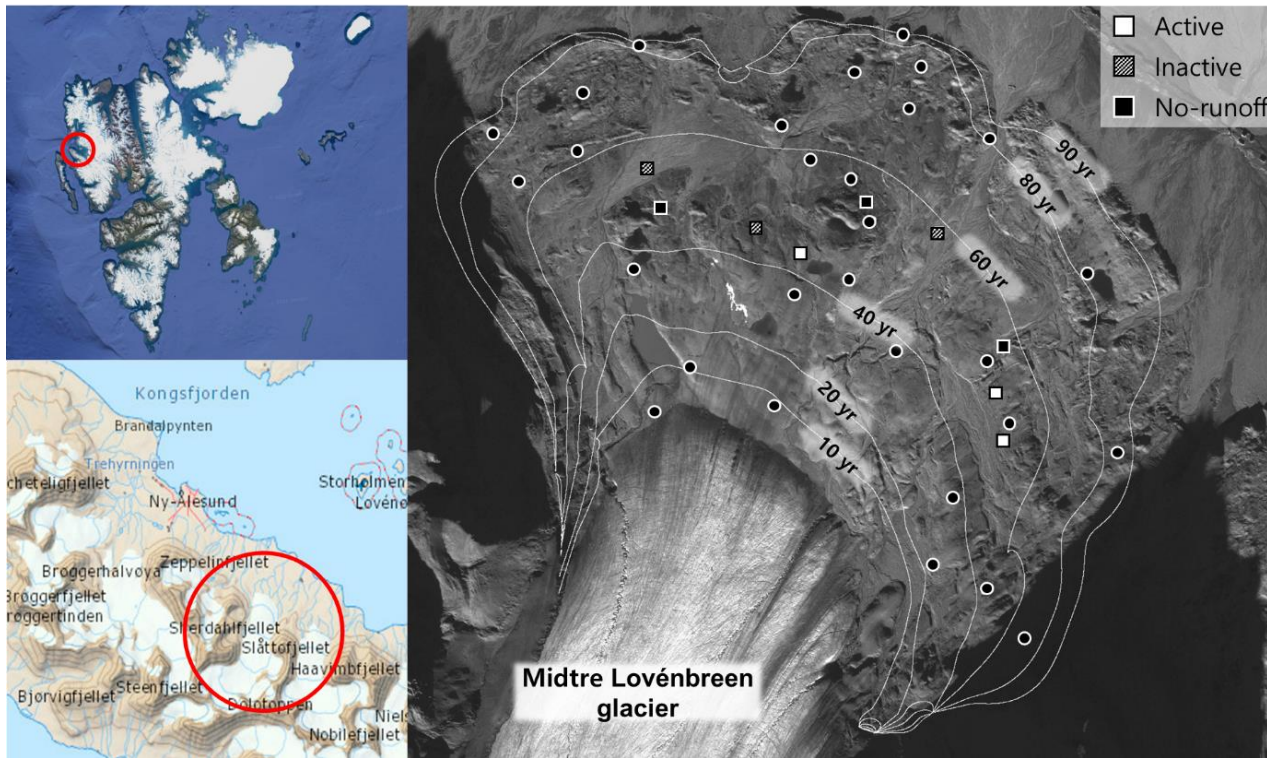


Fig. 1. Sampling points of the Midtre Lovénbreen glacier foreland in northwestern Spitsbergen, Svalbard. The white lines mark the time points of the glacier retreat based on 2014. The circles and squares represent the sampling sites along the chronosequence and glacial-fluvial runoff intensity, respectively.

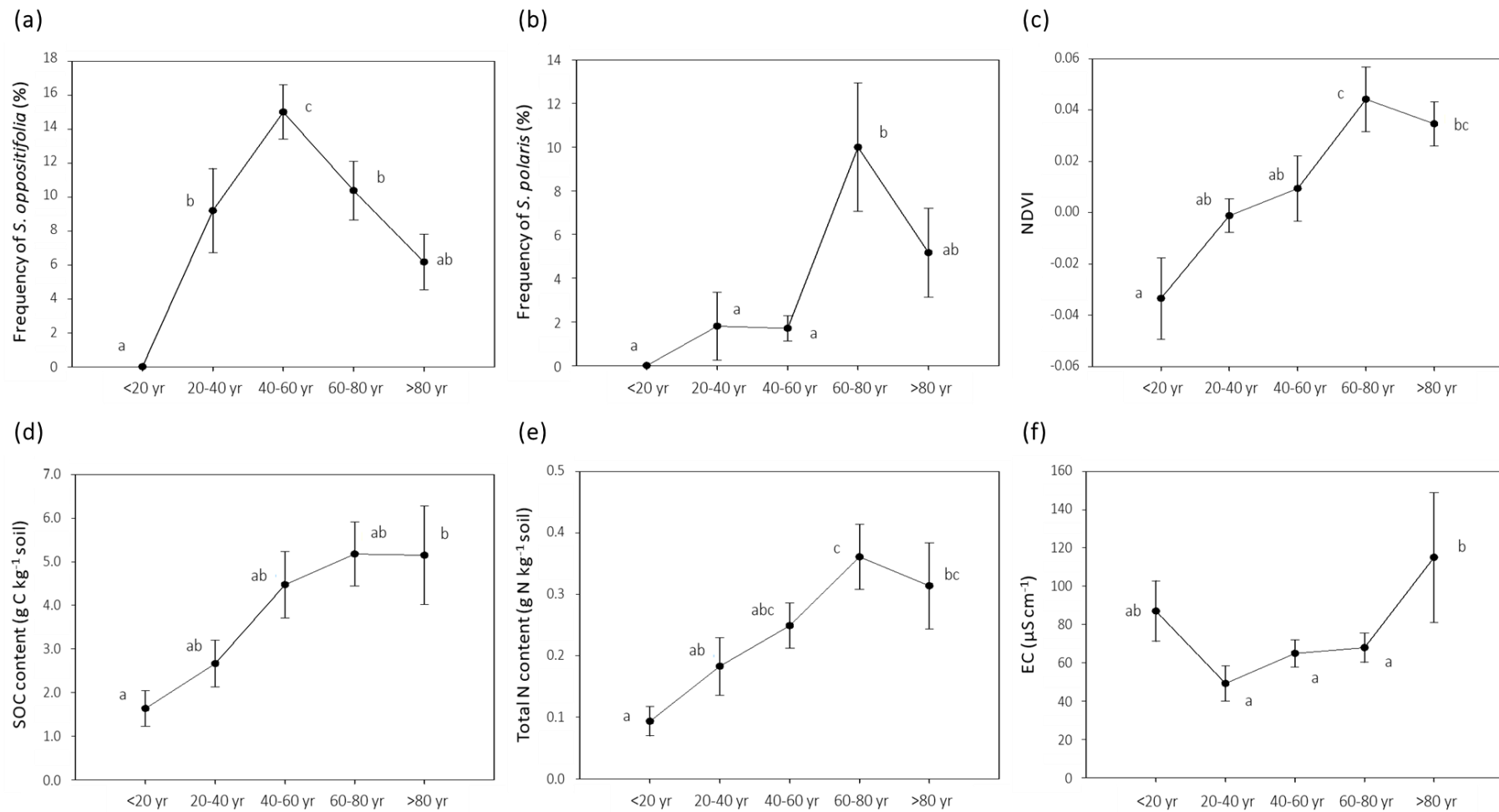


Fig. 2. The changes in the vegetation frequency of *Saxifraga oppositifolia* (a) and *Salix polaris* (b), Normalized Difference Vegetation Index (NDVI; c), soil organic carbon (SOC; d) and total N (e) contents, and electrical conductivity (EC; f) influenced by soil age (soil depth = 0-5 cm). Different letters indicate significant differences at the $p < 0.05$ level using the LSD post-hoc test.

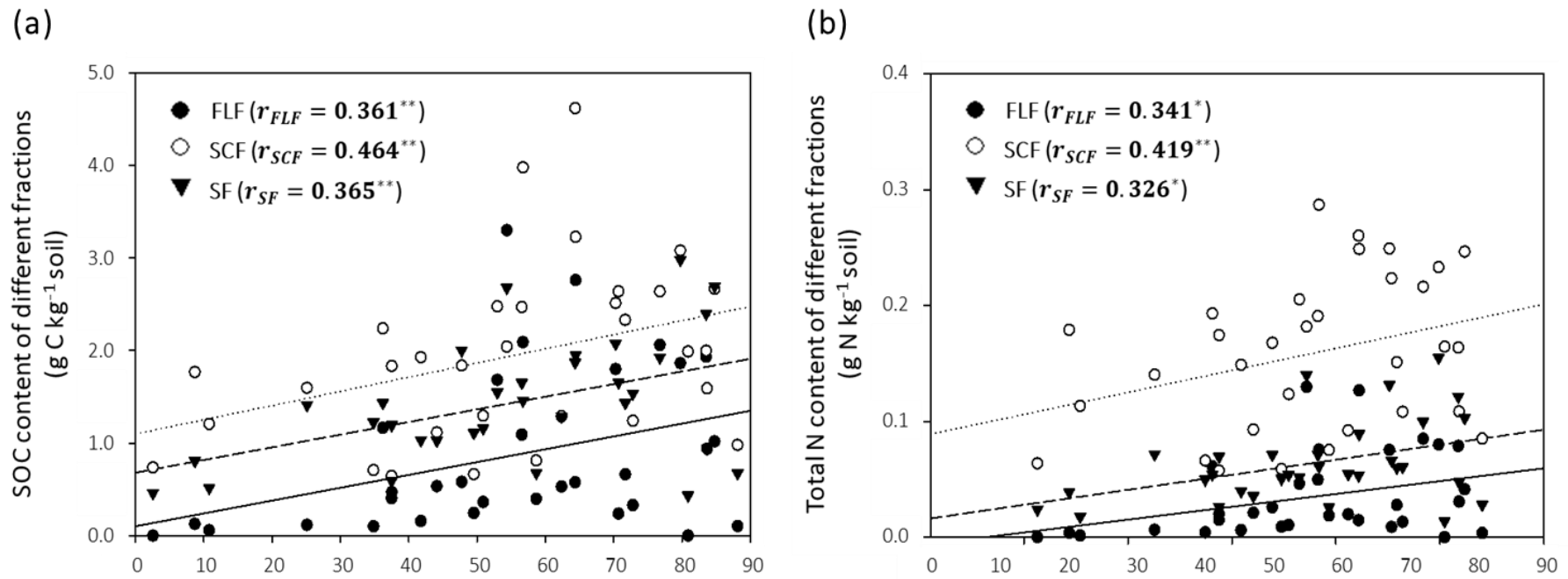


Fig. 3. Simple linear regression analysis of soil organic carbon (SOC; a) and total N (b) contents in the free-light (FLF), silt- and clay-sized (SCF), and sand-sized (SF) fractions (soil depth = 0-5 cm, r = correlation coefficient; ** and * = significance at $p < 0.05$ and $p < 0.10$, respectively).

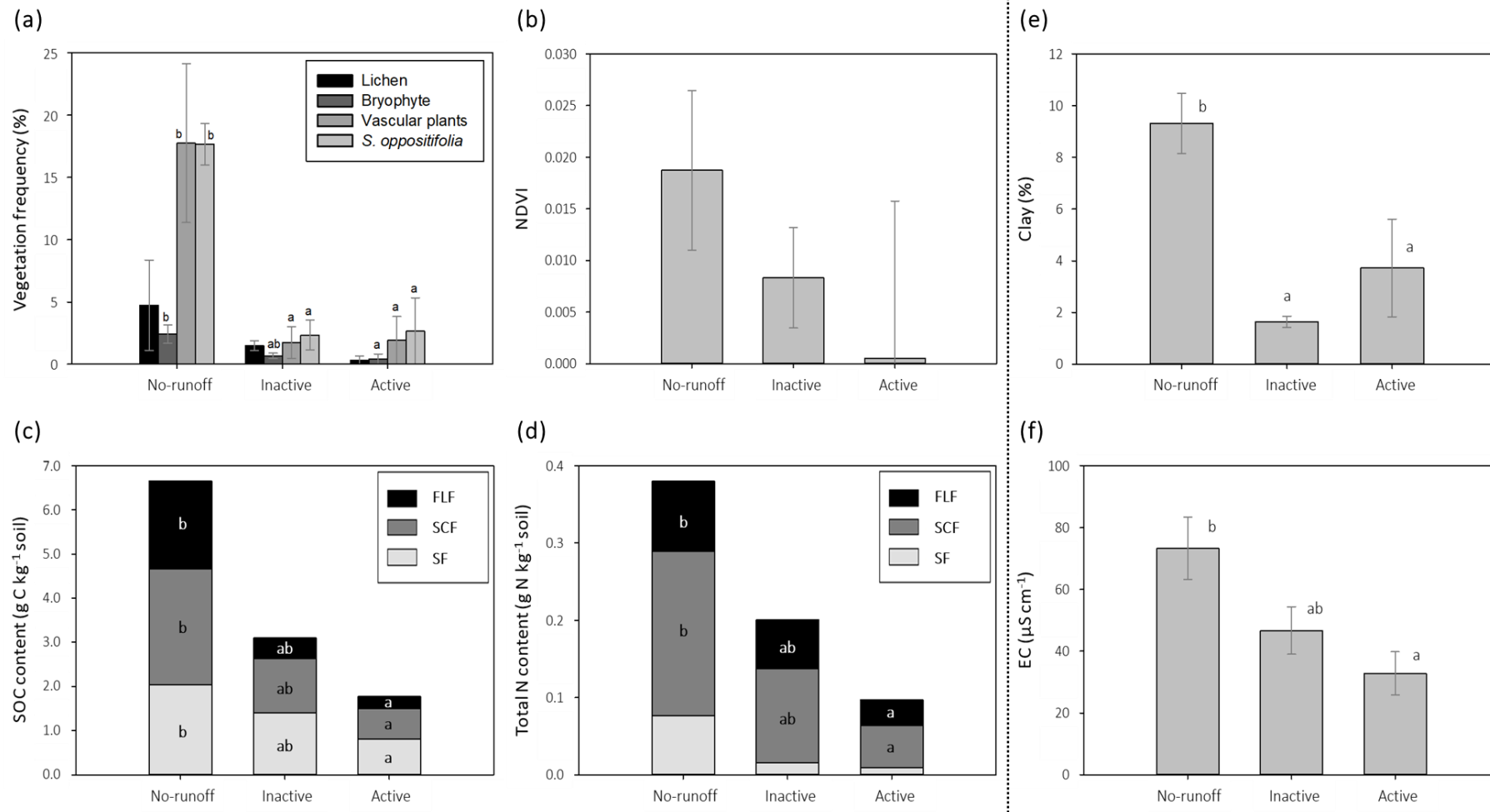


Fig. 4. The changes in the vegetation frequency (a), Normalized Difference Vegetation Index (NDVI; b), soil organic carbon (SOC; c) and total N (d) contents, clay content (e), and electrical conductivity (EC; f) influenced by glacial-fluvial runoff (soil depth = 0-5 cm). Different letters indicate significant differences at the $p<0.05$ level using the post-hoc test.